Unterschiede zwischen den beiden Molekülen der asymmetrischen Einheit festzustellen. Da dies schon ausführlich diskutiert wurde (Post, Kennard & Horn, 1975), soll hier nicht weiter darauf eingegangen werden. Es wurde für nötig befunden, noch mehr Torsionswinkel zu berechnen, als in der erwähnten Arbeit aufgeführt sind.

In Tabelle 6 sind die Kleinste-Quadrate-Ausgleichsebenen durch die Benzolringe charakterisiert. Die Unterschiede in den Koeffizienten der Ebenengleichungen der Bromid- und der Chloridstruktur sind nicht weiter verwunderlich, da ja auch die Zellkonstanten nicht gleich sind. Man beachte aber die in beiden Verbindungen sehr ähnlichen Abstände der Atome von den Ausgleichsebenen.

Hiermit ist gezeigt, dass die beiden Verbindungen isomorph kristallisieren, obwohl sich in der asymmetrischen Einheit jeweils zwei Moleküle mit unterschiedlicher Konformation zusammenfinden müssen.

Literatur

COHEN, N. C. (1971). Persönliche Mitteilung. Centre de Recherches Roussel Uclaf, Romainville, Frankreich.

GERMAIN, G., MAIN, P. & WOOLFSON, M. M. (1970). *Acta Cryst.* B**26**, 274–285.

GERMAIN, G. & WOOLFSON, M. M. (1968). *Acta Cryst.* B**24**, 91–96.

HOPPE, W. (1965). *Angew. Chem.* **77**, 484–492.

International Tables for X-ray Crystallography (1962). Vol. III, pp. 201–206, Birmingham: Kynoch Press.

JOHNSON, C. K. (1965). *ORTEP*. Bericht ORNL-3794, in leicht geänderter Form. Oak Ridge National Laboratory, Tennessee.

KITAIGORODSKY, A. I. (1973). *Molecular Crystals and Molecules*. New York, London: Academic Press.

LÜDECKE, H. & PAULUS, E. F. (1977). *Programm zur Berechnung von Packungskoeffizienten*, Hoechst AG, Frankfurt am Main.

MAIN, P., WOOLFSON, M. M. & GERMAIN, G. (1969). *LSAM, A System of Computer Programs for the Automatic Solution of Centrosymmetric Crystal Structures*. Univ. York, England, und Louvain, Belgien.

PAULING, L. (1964). *Die Natur der chemischen Bindung*, S. 475. Weinheim/Bergstrasse: Verlag Chemie.

POST, M. L., KENNARD, O. & HORN, A. S. (1975). *Acta Cryst.* B**31**, 1008–1013.

SCHINDLER, W. & HÄFLIGER, F. (1954). *Helv. Chim. Acta*, **37**, 472–483.

Acta Cryst. (1978). B**34**, 1947–1956

Single-Crystal Structures and Electron Density Distributions of Ethane, Ethylene and Acetylene.
I. Single-Crystal X-ray Structure Determinations of Two Modifications of Ethane

BY GERARD J. H. VAN NES AND AAFJE VOS

Laboratorium voor Structuurchemie, Rijksuniversiteit Groningen, Nijenborgh 16, 9747 *AG, Groningen, The Netherlands*

(*Received* 7 *November* 1977; *accepted* 1 *January* 1978)

The (plastic) modification of crystalline C_2H_6 at 90 K is cubic, $a = 5{\cdot}304$ (2) Å, space group $Im3m$, $Z = 2$. Anisotropic refinement with 23 independent observed reflexions with $\sin\theta/\lambda \leq 0{\cdot}58$ Å^{-1} gives $R_w = 0{\cdot}026$. The modification at 85 K is monoclinic, $a = 4{\cdot}226$ (3), $b = 5{\cdot}623$ (4), $c = 5{\cdot}845$ (4) Å, $\beta = 90{\cdot}41$ (6)°, space group $P2_1/n$, $Z = 2$. The crystal used shows twinning about (001) with twinning ratio 4:1. Anisotropic refinement with 610 independent observed reflexions with $\sin\theta/\lambda \leq 0{\cdot}81$ Å^{-1} gives $R_w = 0{\cdot}052$. In the plastic modification the molecules are not randomly distributed around their inversion centres. In the monoclinic modification the C—C direction of the molecule is fixed, $\bar{u}^2(C) = 0{\cdot}031$ Å^2, and preferred positions of the H atoms can be distinguished clearly. Both observed structures are essentially different from the hexagonal structure proposed earlier for solid ethane by Mark & Pohland (1925).

1. Introduction

The present paper is part of a series of papers on the determination of the crystal structures and electron density distributions in single crystals of ethane, ethylene and acetylene by X-ray diffraction. In this article we describe the structure determination of two solid phases of C_2H_6 at temperatures above 85 K. Structure determinations of ethane at lower temperatures (preferably He temperatures), to measure the electron density distributions more accurately, are planned for the near future.

In the literature contradictory information is available on the symmetry of solid ethane. Wyckoff (1966) reports a hexagonal structure ($P6_3/m$ $2/m$ $2/c$, $Z = 2$) at 88 K. This structure was found from optical studies (Wahl, 1914; Mark & Pohland, 1925) of a solid sample of ethane just below the melting point, combined with the structural information obtained by Mark & Pohland (1925) from Debye–Scherrer diagrams taken with Zn, Cu and Cr radiation. According to Mark & Pohland, the powder lines correspond quite well to a hexagonal unit cell with $a = b = 4{\cdot}46$, $c = 8{\cdot}19$ Å, $Z = 2$, $D_x = 0{\cdot}708$ and $D_m = 0{\cdot}694$ g cm^{-3}. No definite conclusion was made concerning the space group ($P6_3/m$ $2/m$ $2/c$ was mentioned as one of the possibilities), but a length between 1·46 and 1·64 Å was reported for the C–C bond.

According to an optical and dilatometric study by Eggers (1975), ethane shows the following transformations:

liquid $\longrightarrow$ isotropic solid $\longrightarrow$ anisotropic solid.
90·27 ± 0·02 K 89·92 ± 0·02 K

P–T diagrams reported at the same time by Straty & Tsumura (1976) confirm the existence of the isotropic phase just below the melting point. PMR measurements by Givens & McCormick (1977) have given temperatures of 90·37 and 89·72 (0·05) K for the above transitions and very narrow lines for the isotropic solid. From his study, Eggers suggests that the isotropic solid is a plastic crystalline form, and that the symmetry of the anisotropic solid is lower than hexagonal. On the basis of IR spectra of the latter phase of C_2D_6, Tejada & Eggers (1976) tentatively proposed a slightly distorted hexagonal structure with two molecules in the unit cell related by either a glide plane or a screw axis. Later work (Eggers, 1977) showed, however, that the IR and Raman spectroscopic evidence against the existence of a centre of symmetry at the molecular site is only very slight.

2. Crystal growth

For our experiments ethane gas, obtained from Matheson Co., with a quoted purity >99·0% was used. The gas was transported into capillary tubes by the method described by van Nes & van Bolhuis (1978). Spherical crystals (ø = 0·595 ± 0·003 mm) were grown *in situ* on the diffractometer in a stream of cold nitrogen gas. The open cooling system described by van Bolhuis (1971) was used. Modifications were applied both to go down to temperatures of 85 K without exceeding a N_2 consumption of about 1·5 l h^{-1}, and to stabilize the low temperatures within 0·1 K.

As described by Eggers (1975), a cubic plastic crystalline phase was found just below the melting point. For this phase single crystals of rather good quality (mosaic spread <0·4°) could be grown relatively easily in the following way. First the sample was solidified by moving the spherical end of the capillary tube into the cold gas stream (van Nes & van Bolhuis, 1978). Thereafter a seed (plastic) crystal was produced by moving the tube from the gas stream. From this point the gradual growth of a single crystal was accomplished in a few seconds by taking the sample (slowly) back into cold gas stream. During the crystal growth, colourless needles were observed at and perpendicular to the liquid–plastic solid interface. After complete solidification, the sample looked perfectly clear without any needle structure. This phenomenon has also been observed by Eggers (1975). The crystal could be kept stable at 90·0 K during the 31 h required for the data collection.

Preliminary experiments showed that a monoclinic phase exists at temperatures lower than 90 K. It appeared, however, to be extremely difficult to obtain a single crystal of high quality for this phase. In most trials on lowering the temperature the plastic crystal suddenly collapsed into a white powder. In more favourable cases (by using a seed crystal produced in the gas stream below 90 K) clear crystals were obtained showing, however, severe cracks. In some scarce cases among a large number of trials, crystals could be grown for which the complete reflexion profiles were observed in an ω scan, with a narrow counter slit, within a scan range of 1·0°. For the crystal used for the intensity measurements, the profiles of the different reflexions consisted of one, two or even three peaks. The width of a single peak was <0·5°. It was possible to index the highest peaks of the reflexion profiles on the basis of a monoclinic cell. Crystal orientation and cell dimensions were chosen so as to obtain these highest peaks in the centre of the scan ranges. The crystal did not show significant changes during the 11 d required for the measurement of the intensities.

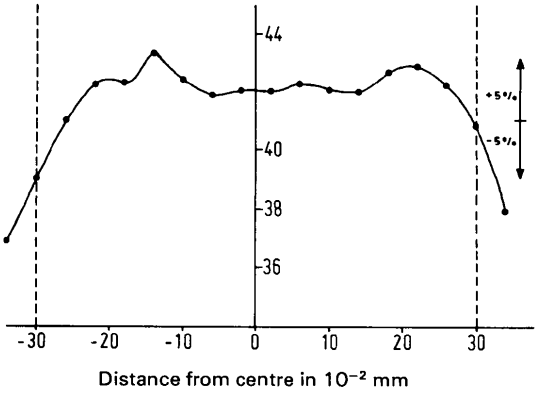

Fig. 1. Intensity profile of the primary beam at the position of the crystal in the plane of incident and scattered wave of the graphite monochromator, as measured for different positions of a pinhole. The profile perpendicular to this plane is flat within the experimental error.

3. Data collection

3.1. *General*

All data were collected on an Enraf–Nonius CAD-4 diffractometer with graphite-monochromatized Mo radiation [same geometry as used by Helmholdt & Vos (1977*b*)]. The intensity distribution in the primary beam is given in Fig. 1. A $\theta/2\theta$ scan with a narrow counter slit for a NaCl reflexion at $\theta = 40°$, gave $\Delta\lambda/\lambda = 0{\cdot}018$ (three times λ_1–λ_2 peak distance). The cell dimensions were determined from θ, φ, ω and κ setting angles measured on the diffractometer; four sets of 24 reflexions were used. The reflexion intensities were calculated from reflexion profiles obtained by the step-scan technique, each scan range being divided into 96 steps. The ω-scan method was applied for both modifications. To avoid icing and to obtain homogeneous cooling of the crystal, the orientation of the capillary tube in the cold gas stream was changed frequently. This was achieved by measuring each reflexion twice in succession, at largely different ψ values. Net intensities were calculated from the profiles by subtracting twice the integrated intensities of the first and last 16 steps from that of the central 64 steps. A correction of $\pm 1{\cdot}5\%$, deduced from the variations of a set of four reference reflexions (measured every 30 min), was made to account for changes in intensity of the primary beam and/or possible changes in the reflecting power of the crystal.

A set of I values for the independent reflexions was obtained by averaging the I values of collected equivalent reflexions. For the plastic phase, $\sigma(I)$ for each mean intensity was calculated from the variations of the intensities of the equivalent reflexions. For the monoclinic phase we used $\sigma_c(I) = [\langle\sigma_{ic}^2\rangle/n]^{1/2}$ where σ_{ic} is the standard deviation due to counting statistics for an individual reflexion i of an equivalent set of n reflexions. The intensities were corrected for Lorentz and polarization effects.

3.2. *Plastic modification*

All reflexions in reciprocal space up to $\sin\theta/\lambda = 0{\cdot}58$ Å^{-1}, including possible systematic extinctions, were collected at two ψ values at 90 K with a scan range of $(1{\cdot}00 + 1{\cdot}00\tan\theta)°$ plus a 25% background region on each side and slit width of $(0{\cdot}46 + 2{\cdot}06\tan\theta)°$. For $\theta > 25°$, the intensities were negligible. The reflexion symmetry and systematic extinctions for the 1059 measured reflexion intensities agree with space group $Im3m$, which is identical with that of the high-pressure plastic modification of C_2D_4 (Press & Eckert, 1976). From the setting angles we obtained $a = 5{\cdot}304$ (2) Å. The b.c.c. cell contains two equivalent molecules making $D_x = 0{\cdot}669$ g cm^{-3}. From the collected reflexion intensities, average intensities were calculated for 23 independent reflexions with $h + k + l = 2n$. For 18 reflexions $I > 0$ and for only 10 reflexions $I \geq 3\sigma(I)$.

3.3. *Monoclinic modification, twinning*

At 85 K, 5147 reflexion intensities (full reciprocal space, two different ψ values) were collected up to $\sin\theta/\lambda = 0{\cdot}81$ Å^{-1}, with a scan range of $(1{\cdot}70 + 1{\cdot}00\tan\theta)°$ plus a 25% background region on each side, and slit width of $(0{\cdot}46 + 1{\cdot}72\tan\theta)°$. In spite of the measuring temperature of 85 K being only 5° below the melting point, reflexions could be obtained above $\sin\theta/\lambda = 1{\cdot}00$ Å^{-1}, as in the case of C_2H_4, which structure was determined at *ca* 19° below its melting point (van Nes & Vos, 1977). Collection of these high-order peaks for C_2H_6 was not considered worthwhile, because of the not too excellent quality of the crystal. From the setting angles corresponding to the highest peak in the centre of each of the scan ranges, we obtained the cell dimensions $a = 4{\cdot}226$ (3), $b = 5{\cdot}623$ (4), $c = 5{\cdot}845$ (4) Å, $\beta = 90{\cdot}41$ (6)°. With $Z = 2$ we obtained $D_x = 0{\cdot}719$ g cm^{-3}. Because many reflexion profiles showed double or triple peaks, the printed profiles of more than 1000 reflexions with large intensities were studied carefully. Starting from the fact that the majority of the $0kl$ reflexion profiles consist of one peak, the study of the reflexion profiles revealed that the crystal used is twinned about the (001) plane. From Fig. 2, which shows the superposition of the reciprocal lattices of the two twin individuals (called I and II), we see that reflexions hkl(I) lie close to or coincide (for $0kl$) with reflexions $hk\bar{l}$(II). As β deviates only 0·41° from 90°, the maximum separation between hkl(I) and $hk\bar{l}$(II) is only 0·82°, so that in all cases both reflexions fall within the same scan range. From the heights of the pairs of peaks $hk0$(I) and $hk0$(II) observed in the same scan range, the twinning ratio,

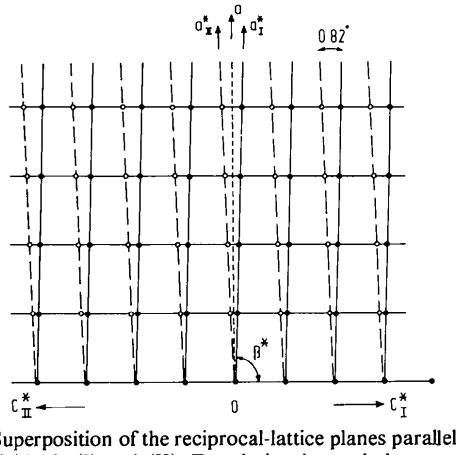

Fig. 2. Superposition of the reciprocal-lattice planes parallel to a^*c^* of individuals (I) and (II). For clarity the angle between a_I^* and a_{II}^* is taken as 3·8° rather than the real value of 0·82°. Lattice points of (I) are given by ● and of II by ○. In all cases neighbouring ● and ○ points lie within a scan region of 0·82°.

m = reflecting power (I)/reflecting power (II), was determined roughly at 4·7. During the refinement of the structure, m was determined more accurately.

The twinning described above does not account for the occurrence of some double $0kl$ peaks and some triple hkl peaks. No strict explanation of the additional peaks, which had low intensities, could be given. We have not corrected for these peaks because refinement with account taken of the monoclinic twinning gives $R_w = 0{\cdot}052$ (§ 5.3). The high consistency between equivalent reflexions (see below) suggests that the additional peaks are (partly) of a systematic character (§ 6.2). Further, the presence of tiny misorientated crystallites, of either the monoclinic or the cubic modification, cannot be excluded. Givens & McCormick (1977), for instance, did not succeed in forming the low-temperature phase completely free from the high-temperature phase for their PMR experiments.

Because of the presence of unexplained weak peaks, peaks with low intensity and not lying at the centre of a scan range were neglected in the determination of the space group. In addition to the monoclinic reflexion symmetry, we found the systematic extinctions $h0l$ for $h + l \neq 2n$ and $0k0$ for $k \neq 2n$ indicating the space group $P2_1/n$. This was confirmed by the results of the structure refinement. The space group is identical with that of the modification of C_2H_4 at 85 K (van Nes & Vos, 1977).

Integrated intensities of the 5147 measured reflexions were calculated as mentioned before. 122 reflexions for which no reliable intensities could be obtained, because of the presence of additional peaks in the background region, were excluded. The remaining reflexions were contracted to a set of 610 independent reflexions. The internal consistency factors are:

$$R_I = \left\{ \sum_{H,i} [I(H,i) - \overline{I(H)}]^2 / \sum_{H,i} I^2(H,i) \right\}^{1/2} = 0{\cdot}036$$

and

$$R_F = \left\{ \sum_{H,i} [F(H,i) - \overline{F(H)}]^2 / \sum_{H,i} F^2(H,i) \right\}^{1/2} = 0{\cdot}034.$$

$I(H,i)$ is the reflexion intensity before Lorentz and polarization correction, H is the independent reflexion index and i indicates the reflexion within an equivalent set. The 610 non-equivalent reflexions include four reflexions with $I < 0$; there are 575 reflexions with $I \geq 3\sigma_c(I)$.

4. Structure determination and refinements for the plastic modification

4.1. *General*

For the calculations the set of programs of the XRAY system (1975) was used. The temperature factor has the form $\exp\{-2\pi^2[(h_i a^I)(h_j a^I) U^{ij}]\}$ where h_i and a^I are, respectively, the reflexion indices and lengths of the reciprocal-unit-cell axes. Scattering factors for spherically symmetric C atoms were taken from Cromer & Mann (1968) and for H from Stewart, Davidson & Simpson (1965). The least-squares function minimized is

$$Q = \sum_H w[F_o(H) - k^{-1}F_c(H)]^2.$$

The residual R_w is defined as $R_w = [\sum w(F_o - F_c)^2 / \sum wF_o^2]^{1/2}$.

No extinction correction (Zachariasen, 1967, 1968) was applied, as in none of the structure determinations was F_o systematically lower than F_c for strong low-order reflexions.

4.2. *Structure models*

From the space group $Im3m$ (No. 229, $I4/m\ \bar{3}\ 2/m$) and $Z = 2$, it follows that the molecules lie at a special position with site symmetry $m3m$. The inversion centres of the molecules were placed at (0,0,0) and $(\frac{1}{2},\frac{1}{2},\frac{1}{2})$. In order to obey the site symmetry, static or dynamic disorder of the molecules around their inversion centres has to be assumed. Several possibilities were scanned to check which model, after anisotropic least-squares refinement, gives the best agreement between observed and calculated structure factors. In all cases the full set of 23 independent reflexions was used with unit weights. For the reflexions with a measured negative intensity $F_o = 0$ was taken. The following models were checked (Table 1 and Fig. 3).

(*A*) $\frac{1}{4}$C atom with anisotropic thermal motion at $[x,x,x]$, which results in a fractional coordinate $x = 0{\cdot}0767\ (25)$ with C–C = 1·409 Å.

(*B*) Homogeneous distribution of two C and six H atoms around the molecular centre, the spherical surfaces being smeared out by anisotropic thermal motion. The radii of the C and H spheres were calculated from the geometry of the C_2H_6 molecule

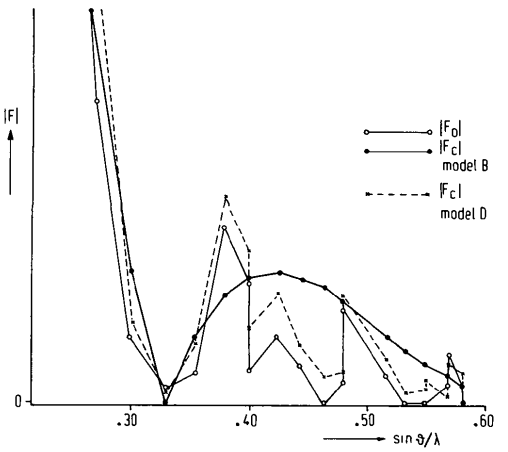

Fig. 3. Plastic modification. Comparison between $|F_o|$ and $|F_c|$ for different models for reflexions with $\sin\theta/\lambda > 0{\cdot}27$ Å^{-1} (see also text and Table 1).

Table 1. *Observed and calculated structure factors for the plastic modification*

Models *A*, *B*, *C* and *D* are described in the text. The thermal parameters (Å²) are multiplied by 10^2. Numbers in parentheses here and elsewhere in this paper are the estimated standard deviations in the least significant digits

h k l	sin θ/λ (Å^{-1})	F_o	*A*	*B*	*C*	*D*
1 1 0	0·133	51·14 (59)	51·35	51·91	51·46	51·52
2 0 0	0·189	22·80 (5)	21·79	20·19	21·87	21·88
2 1 1	0·231	7·43 (1)	8·57	8·22	7·45	7·27
2 2 0	0·267	2·58 (1)	2·76	3·36	3·72	3·30
3 1 0	0·298	0·59 (3)	0·38	1·16	0·99	0·70
2 2 2	0·327	0·14 (11)	−0·61	0·08	−0·59	−0·12
3 2 1	0·353	0·27 (4)	−0·93	−0·58	−0·64	−0·53
4 0 0	0·377	1·50 (3)	−0·93	−0·93	−1·38	−1·78
3 3 0	0·400	0·25 (9)	−0·81	−1·08	−0·77	−0·65
4 1 1	0·400	1·04 (2)	−0·81	−1·08	−1·10	−1·31
4 2 0	0·422	0·59 (4)	−0·66	−1·12	−0·88	−0·96
3 3 2	0·442	0·34 (6)	−0·38	−1·08	0·22	0·50
4 2 2	0·462	0·00 (22)	−0·32	−1·00	−0·33	−0·24
4 3 1	0·481	0·19 (8)	−0·24	−0·89	−0·33	−0·27
5 1 0	0·481	0·82 (4)	−0·31	−0·89	−0·68	−0·93
5 2 1	0·516	0·25 (7)	−0·14	−0·58	−0·31	−0·39
4 4 0	0·533	0·00 (29)	−0·09	−0·46	−0·14	−0·10
4 3 3	0·550	0·00 (27)	0·01	−0·35	0·16	0·21
5 3 0	0·550	0·00 (27)	−0·06	−0·35	−0·14	−0·15
4 4 2	0·566	0·18 (12)	0·00	−0·27	0·02	0·06
6 0 0	0·566	0·43 (16)	−0·06	−0·27	−0·23	−0·37
5 3 2	0·581	0·00 (22)	−0·00	−0·19	−0·02	−0·01
6 1 1	0·581	0·17 (15)	−0·04	−0·19	−0·15	−0·24
R_w			0·036	0·060	0·032	0·026
C–C			1·409	–	1·388	1·409
U_{ii}(C)			25 (2)	10 (2)	19 (7)	17 (4)
$\lvert U_{ij}$(C)$\rvert$			4 (1)	–	2 (2)	1 (1)
U_{ii}('H')			–	–	70 (119)	63 (36)
$\lvert U_{ij}$('H')$\rvert$			–	–	34 (58)	31 (18)

obtained by electron diffraction (Kuchitsu, 1968) (Fig. 4).

(*C*) Apart from the usual anisotropic motion, $\frac{1}{4}$[C–C] along $[x,x,x]$ with, on either side of the molecule, a random distribution of $\frac{3}{4}$H atoms over a circle of radius r around $[x,x,x]$. This corresponds to a free rotation of the molecule around C–C. x_C was constrained at 0·0767 (see *A*). For the scattering function of the $\frac{3}{4}$H atoms, the well known formula for a spherically symmetric atom rotating around an axis **q** was taken (*International Tables for X-ray Crystallography*, 1959):

$$f(S) = \tfrac{3}{4} f_H(S) \exp\{2\pi i(hx_q + ky_q + lz_q)\} J_0(2\pi tr).$$

$f_H(S)$ is the usual scattering factor for H; x_q,y_q,z_q is the point of intersection of **q** with the plane of the circle; r = radius of the circle; t = distance of the endpoint of **S** to a vector parallel to **q** going through the reciprocal-space origin; J_0 is the zero-order Bessel function. For the radius r the literature value 1·019 Å (Fig. 4) was taken; x_q,y_q,z_q was put at a distance of 0·368 Å from the C atom (literature value reduced by 8%, which is the relative libration shortening found for C–C in model *A*).

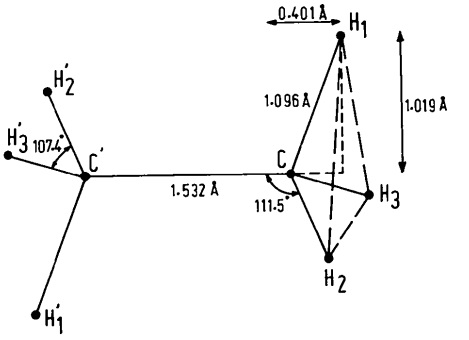

Fig. 4. C_2H_6 geometry from electron diffraction (Kuchitsu, 1968). Standard deviations in bond lengths 0·002 Å, and in angles 0·3°. Symmetry molecule $\bar{3}$.

(*D*) A model describing in an approximate way a strong libration of the molecules around their centres with preferred C–C directions along $[x,x,x]$. The H atoms are assumed to be smeared out so strongly that the maximum density of the three H atoms of a CH_3 group lies at $[x,x,x]$. We therefore used the linear model $\frac{1}{4}$[(3H)–C–C–(3H)] along $[x,x,x]$; x_C was constrained at 0·0767 (see *A*), x(3H) = x_q,y_q,z_q of model *C*.

4.3. *Conclusion*

From Table 1 and Fig. 3 we see that model *D* gives the best agreement between F_o and F_c. We can conclude that the molecules do not rotate freely nor are they distributed randomly around their inversion centres. An $[F_o(H) - F_c(H)]$ difference map after refinement with model *D* gives a value of 0·28 e Å^{-3} at the (fixed) centres of the C–C bonds. The next-highest absolute values are maxima of 0·16 e Å^{-3} at [111] at a distance of *ca* 2·3 Å from the centre.

5. Structure determination and refinement for the monoclinic modification

5.1. *Approximate structure model*

From the space group $P2_1/n$ with $Z = 2$, it follows that the molecules lie at a twofold position with symmetry $\bar{1}$. No disorder need be assumed, if for the molecules a staggered conformation with an inversion centre is adopted. Reasonable starting positions for C were obtained from the assumption that the structure of C_2H_6 has some analogy with that of C_2H_4 (van Nes & Vos, 1977). Approximate positions of the H atoms were deduced from difference Fourier syntheses after anisotropic refinement of the C atoms.

5.2. *Refinement, twinning, weighting scheme*

In the refinement the full set of 610 independent reflexions was used. Further general remarks are as for the plastic modification. In the first few least-squares cycles, $w = 1$ was taken and the twinning was neglected. Refinement with only C atoms results in $R_w = 0{\cdot}178$ decreasing to 0·125 by including the H atoms (anisotropic temperature factors for all atoms).

As a result of the twinning, the intensities measured in the scans of the reflexions hkl(I) and $hk\bar{l}$(I) (Fig. 2) are given by:

$$I_{\rm exp}(\text{at } hkl,\text{I}) = \frac{m}{m+1} I(hkl,\text{I}) + \frac{1}{m+1} I(hk\bar{l},\text{II}) \qquad (1)$$

$$I_{\rm exp}(\text{at } hk\bar{l},\text{I}) = \frac{1}{m+1} I(hkl,\text{II}) + \frac{m}{m+1} I(hk\bar{l},\text{I}) \qquad (2)$$

with twinning ratio $m = I(hkl,\text{I})/I(hkl,\text{II})$.

Equations (1) and (2) show that the intensities for the reflexions 0kl and hk0 are not affected by the twinning because $I(0kl) = I(0k\bar{l})$, and $I(hkl) = I(hk\bar{l})$ when $l = \bar{l} = 0$. Therefore, anisotropic refinements including both C and H were carried out with the 64 reflexions 0kl and with the 46 reflexions hk0, both with $w = 1$. Residuals $R_w = 0{\cdot}037$ and 0·024, respectively, were obtained with reasonable parameters for the C and H atoms, showing that the adopted model is essentially correct. Thereafter the twinning parameter m was determined by calculating $I(hkl,\text{I})$ and $I(hk\bar{l},\text{I})$ from (1) and (2) for different values of m and performing anisotropic least-squares refinements on $F(hkl,\text{I})$. R_w reached a minimum value of 0·049 for $m = 4{\cdot}0$.

For $w = 1$, $\langle w(|F_o| - |F_c|)^2 \rangle$ with F_o calculated from (1) and (2) varied systematically as a function of $|F_o|$ and $\sin\theta$. Therefore, an analytical weighting scheme was chosen to reduce these variations as much as possible. No account was taken of the earlier calculated standard deviations of the individual reflexions, as these standard deviations were assumed to be small in comparison with the errors due to the presence of additional peaks (§ 3.3) or to a possible error in m. The weights chosen were $w = w_1 w_2$ with:

$$w_1 = 0{\cdot}007(-0{\cdot}129 \sin\theta + 0{\cdot}061)^{-1} \quad \text{for } \sin\theta \le 0{\cdot}419,$$
$$w_1 = 1 \quad \text{for } \sin\theta > 0{\cdot}419;$$
$$w_2 = 0{\cdot}0034(-0{\cdot}011 F_o + 0{\cdot}010)^{-1} \quad \text{for } F_o \le 0{\cdot}618,$$
$$w_2 = 1 \quad \text{for } F_o > 0{\cdot}618.$$

In the determination of the weighting scheme, the very strong reflexions 101 and 10$\bar{1}$ with, in comparison with the other reflexions, large $|F_o - F_c|$ values, were not considered. The relative difference $\Delta F/F$ is smaller than 7% for these two reflexions.

Use of the weighting scheme minimized R_w (0·052) for $m = 4{\cdot}2$. It was found, however, that the small change in m from 4·0 to 4·2 did not have a significant influence on the parameters and electron density distributions.

5.3. *Final stage of the refinement and calculation of electron density distributions*

The results are summarized in Tables 2 and 3. For all refinements we used anisotropic temperature factors, a twinning ratio $m = 4{\cdot}2$ and spherically symmetric non-bonded atoms in the structure model. Because of the uncertainties in the intensities due to the twinning, advanced refinements with non-spherical atoms

Table 2. *Results of refinements with* C *atoms only*

For description of models see text. Thermal parameters (Å^2) are multiplied by 10^4.

Model	$A1(w=1)$	$A2(w=w_1w_2)$	$A3$('lit.')	Model	$A1(w=1)$	$A2(w=w_1w_2)$	$A3$('lit.')
x	−0·03808 (52)	−0·03841 (36)	−0·03890 (16)	U_{11}	360 (10)	336 (6)	336 (6)
y	0·09539 (41)	0·09472 (27)	0·09592 (12)	U_{22}	343 (10)	318 (6)	319 (6)
z	−0·08801 (37)	−0·08779 (26)	−0·08890 (12)	U_{33}	357 (10)	329 (6)	329 (6)
C–C	1·519 (5)Å	1·513 (4) Å	1·532 (2) Å	U_{12}	3 (8)	2 (5)	1 (5)
R_w	0·141	0·121	0·125	U_{13}	−13 (8)	−7 (4)	−7 (4)
				U_{23}	46 (8)	44 (5)	44 (5)

Table 3. *Results of refinements with* C *and* H *atoms*

For description of models see text. Thermal parameters (Å²) are multiplied by 10^2. Apart from C–H, the standard deviations in *B*3('lit') are comparable with those of *B*2.

Model	*B*1($w = 1$)	*B*2($w = w_1 w_2$)	*B*3('lit.')	Model	*B*1($w = 1$)	*B*2($w = w_1 w_2$)	*B*3('lit.')
x(C)	−0·03792 (21)	−0·03848 (16)	−0·03890	C–C	1·506 (2)	1·510 (2)	1·532 (2)
y(C)	0·09429 (16)	0·09447 (12)	0·09592	C–H(1)	1·003 (14)	0·970 (17)	1·096 (2)
z(C)	−0·08746 (15)	−0·08768 (12)	−0·08890	C–H(2)	0·941 (13)	0·917 (16)	1·096 (2)
x(H1)	0·0612 (28)	0·0562 (34)	0·0695	C–H(3)	0·996 (16)	0·993 (15)	1·096 (2)
y(H1)	0·0561 (22)	0·0560 (27)	0·0490	C–C–H(1)	111·0 (7)	110·7 (9)	109·5
z(H1)	−0·2384 (21)	−0·2338 (26)	−0·2525	C–C–H(2)	113·8 (8)	113·0 (9)	111·8
x(H2)	0·0461 (32)	0·0403 (36)	0·0560	C–C–H(3)	110·1 (7)	110·2 (9)	108·8
y(H2)	0·2448 (24)	0·2411 (28)	0·2698	H(1)–C–H(2)	103·3 (1·0)	105·3 (1·3)	107·1
z(H2)	−0·0514 (21)	−0·0494 (25)	−0·0388	H(1)–C–H(3)	111·1 (1·0)	110·5 (1·2)	111·4
x(H3)	−0·2714 (36)	−0·2712 (35)	−0·2965	H(2)–C–H(3)	107·3 (1·1)	107·1 (1·3)	108·3
y(H3)	0·1130 (23)	0·1118 (29)	0·1114				
z(H3)	−0·1033 (21)	−0·1045 (26)	−0·1052	R_w	0·049	0·052	0·070
U_{11}(C)	3·12 (4)	3·15 (3)	3·23 (4)	U_{11}(H2)	7·3 (10)	6·3 (10)	10·2 (18)
U_{22}(C)	3·02 (4)	2·97 (3)	3·09 (4)	U_{22}(H2)	3·8 (8)	4·4 (8)	5·3 (13)
U_{33}(C)	3·14 (4)	3·07 (3)	3·17 (4)	U_{33}(H2)	6·2 (9)	5·7 (9)	7·4 (14)
U_{12}(C)	0·01 (3)	0·00 (2)	0·00 (3)	U_{12}(H2)	−0·3 (7)	0·6 (8)	0·3 (13)
U_{13}(C)	−0·08 (3)	−0·07 (2)	−0·07 (2)	U_{13}(H2)	−4·8 (8)	−3·2 (8)	−5·4 (13)
U_{23}(C)	0·36 (3)	0·39 (2)	0·41 (3)	U_{23}(H2)	2·1 (7)	1·2 (7)	1·4 (12)
U_{11}(H1)	5·5 (8)	5·9 (9)	6·8 (13)	U_{11}(H3)	8·0 (11)	5·0 (9)	7·8 (15)
U_{22}(H1)	5·3 (9)	5·2 (9)	6·3 (14)	U_{22}(H3)	6·0 (10)	6·8 (11)	7·5 (16)
U_{33}(H1)	4·1 (7)	5·1 (9)	5·8 (12)	U_{33}(H3)	6·0 (9)	6·8 (10)	7·4 (15)
U_{12}(H1)	0·5 (7)	1·0 (8)	0·9 (11)	U_{12}(H3)	1·0 (9)	1·1 (8)	0·3 (14)
U_{13}(H1)	−0·5 (7)	−0·9 (7)	−0·9 (11)	U_{13}(H3)	−1·7 (8)	−0·9 (8)	−2·3 (12)
U_{23}(H1)	1·7 (7)	1·4 (8)	1·9 (11)	U_{23}(H3)	3·6 (8)	3·1 (9)	2·8 (13)

(Stewart, 1976) and with higher cumulants in the temperature factor to account, for instance, for the librational character of the thermal motion (Johnson, 1969) were not considered worthwhile. The following refinements were performed.

(*A*) Refinements with C atoms only: (1) no constraints, $w = 1$; (2) no constraints, $w = w_1 w_2$; (3) direction C–C as in *A*2 and distance C–C constrained at the literature value 1·532 Å, $w = w_1 w_2$.

(*B*) Refinements with both C and H atoms: (1) no constraints, $w = 1$; (2) no constraints, $w = w_1 w_2$;* (3) positions of C constrained at *A*3 values. First C–H directions obtained by refinement of H positions and temperature factors of C and H. Thereafter C–H bonds constrained at literature values in the directions obtained, and refinement of C and H thermal parameters only.

For the unconstrained refinement *B*2, the C–C bond length obtained (Table 3) is shorter than the gas-phase value of 1·532 Å. This shortening can be ascribed to librational motion and to neglect of the effects of chemical bonding during the refinement. No estimate of the librational shortening could be made, as a rigid-body analysis (Cruickshank, 1956) with the program *TMA* (Shmueli, 1972) showed that the ethane molecule cannot be described as a rigid body.

* A list of structure factors has been deposited with the British Library Lending Division as Supplementary Publication No. SUP 33399 (4 pp.). Copies may be obtained through The Executive Secretary, International Union of Crystallography, 13 White Friars, Chester CH1 1NZ, England.

The above errors in the bond lengths are eliminated in model *B*3 where gas electron diffraction values (Kuchitsu, 1968) have been taken for these lengths. The angles have been adjusted to the X-ray data, as the bending force constants are considerably smaller than the stretching force constants (Herzberg, 1966): C–H $4{\cdot}79 \times 10^5$, C–C $4{\cdot}50 \times 10^5$, C–C–H $0{\cdot}66 \times 10^5$, H–C–H $0{\cdot}55 \times 10^5$ dyn cm^{-1}. Differences in bond angles of up to 4° from the literature values were observed. In our opinion the coordinates of model *B*3 are the best geometrical description of the structure. The fact that for refinement *B*2 the average values for C–C–H and H–C–H are almost equal to the gas diffraction values does not necessarily mean that for the crystal the angles found in *B*2 are better than those of *B*3.

Sections of the $[F_o - F_c$ (model)] difference density distributions were calculated for all the structure models obtained. In all cases the F_c values are based on non-bonded spherically symmetric atoms. No essential differences were found between maps for all observed reflexions and for reflexions with $|F| > 5\sigma(|F|)$ only; differences between maps based on refinements with $w = 1$ and $w = w_1 w_2$ could be ascribed to the differences in the C parameters. In § 6.3 the discussion will be restricted to maps obtained after refinements with $w = w_1 w_2$ and including all observed reflexions. Some sections are shown in Fig. 9. Standard deviations for general positions in these maps were estimated by considering the density at positions far removed from atoms and chemical bonds. The D(max) values in these

regions were considered as $3\sigma(D)$, giving $\sigma(D) = 0.025$ e Å^{-3}. At the inversion centres, the standard deviation is larger and is estimated at $\sigma(D, \text{centre}) = 0.038$ e Å^{-3}. Moreover, systematic errors can occur, especially as a result of possible errors in the scale and twinning factors and neglect of TDS corrections (Helmholdt & Vos, 1977*a*).

6. Discussion

6.1. *Description of the structures*

(*a*) *Cubic modification*

The cubic modification with symmetry *Im3m*, has two molecules in the unit cell at (0,0,0) and $(\frac{1}{2},\frac{1}{2},\frac{1}{2})$. The distance between the molecular centres along [111] is 4·593 Å and along [100] 5·304 Å. From § 4.2 we see that the strong orientational disorder present in this plastic crystal is described quite well by model *D* (Fig. 3, Table 1).

(*b*) *Monoclinic modification*

The packing of the molecules in the monoclinic modification is shown in Fig. 5 (*ORTEP* program, Johnson, 1970). The two molecules in the cell lie at the inversion centres (0,0,0) and $(\frac{1}{2},\frac{1}{2},\frac{1}{2})$ and have a staggered conformation. The distance between the molecular centres along [111], [$\bar{1}$11], [100], [010] and [001] is 4·563, 4·582, 4·226, 5·623 and 5·845 Å respectively. The first two values are only slightly different from the value 4·594 Å in the cubic modification. Apart from differences up to 4° in the valence angles, the geometry of the molecules in the crystal is assumed to be the same as in the gaseous phase (§ 5.3 model *B*3). Geometrical data of the structure based on model *B*3 are listed in Tables 3 and 4. The structure is packed quite loosely as there are no intermolecular distances shorter than the sum of the relevant van der Waals radii ($r_C = 1.7$, $r_H = 1.2$ Å). The two shortest H···H distances (2·46 and 2·55 Å) are between the $(10\bar{1})_n$ planes and almost perpendicular to [101]. The C–C bonds make an angle of 13·7° with these planes. The thermal motion of the C atoms is almost isotropic and not very high [$\overline{u^2}$(C) = 0·031 Å^2 for model *B*2]. For the H atoms an additional r.m.s. libration of *ca* 13° around the C–C bond and some riding (non-rigid body) motion is found.

Table 4. *Intramolecular distances, short non-bonding distances* (Å) *and orientation of* C–C *bonds*

Distances shorter than the sum of the relevant van der Waals radii [r(C) = 1·7, r(H) = 1·2 Å; Pauling (1960)] plus 0·6 Å are listed for the structure of model *B*3 (see text). Standard deviations in bond lengths are given in Fig. 4; for the non-bonded distances the standard deviations are estimated at 0·015 Å for C···H and 0·02–0·03 Å for H···H.

Symmetry code for atom *A*

$A(n,\text{i}) \equiv A(n; x,y,z)$	$A(n,\text{vi}) \equiv A(n; x+\frac{1}{2}, y+\frac{1}{2}, z+\frac{1}{2})$
$A(n',\text{i}) \equiv A(n; \bar{x}, \bar{y}, \bar{z})$	$A(n,\text{vii}) \equiv A(n; x-\frac{1}{2}, y+\frac{1}{2}, z+\frac{1}{2})$
$A(n,\text{ii}) \equiv A(n; x+1, y, z)$	$A(n,\text{viii}) \equiv A(n; x+\frac{1}{2}, y+\frac{1}{2}, z-\frac{1}{2})$
$A(n,\text{iii}) \equiv A(n; x-1, y, z)$	$A(n,\text{ix}) \equiv A(n; x-\frac{1}{2}, y+\frac{1}{2}, z-\frac{1}{2})$
$A(n,\text{iv}) \equiv A(n; x, y+1, z)$	$A(n,\text{x}) \equiv A(n; x+\frac{1}{2}, y-\frac{1}{2}, z-\frac{1}{2})$
$A(n,\text{v}) \equiv A(n; x, y, z-1)$	$A(n,\text{xi}) \equiv A(n; x-\frac{1}{2}, y-\frac{1}{2}, z-\frac{1}{2})$

Intramolecular distances

C(1,i)–C(1′,i)	1·532	H(1,i)–H(2,i)	1·76
C(1,i)–H(1,i)	1·096	H(1,i)–H(3,i)	1·81
C(1,i)–H(2,i)	1·096	H(1,i)–H(1′,i)	3·06
C(1,i)–H(3,i)	1·096	H(1,i)–H(2′,i)	2·53
C(1,i)–H(1′,i)	2·16	H(1,i)–H(3′,i)	2·47
C(1,i)–H(2′,i)	2·19	H(2,i)–H(3,i)	1·78
C(1,i)–H(3′,i)	2·15	H(2,i)–H(2′,i)	3·11
		H(2,i)–H(3′,i)	2·52
		H(3,i)–H(3′,i)	3·05

Intermolecular distances

C(1,i)–C(1,vi)	3·99	H(1,i)–H(1′,v)	3·00
C(1,i)–C(1,vii)	4·01	H(1,i)–H(2,viii)	2·85
C(1,i)–C(1′,ix)	3·82	H(1,i)–H(2,ix)	2·92
C(1,i)–H(1,vii)	3·26	H(1,i)–H(2′,x)	2·55
C(1,i)–H(1′,viii)	3·36	H(1,i)–H(3,ii)	2·83
C(1,i)–H(2,ix)	3·22	H(1,i)–H(3,viii)	2·87
C(1,i)–H(2′,xi)	3·33	H(1,i)–H(3′,xi)	2·84
C(1,i)–H(3,ii)	3·14	H(2,i)–H(2′,iv)	2·67
C(1,i)–H(3′,iii)	3·25	H(2,i)–H(3,ii)	2·91
C(1,i)–H(3,vi)	3·42	H(2,i)–H(3,vi)	2·69
C(1,i)–H(3′,ix)	3·47	H(2,i)–H(3′,ix)	3·03
		H(3,i)–H(3′,iii)	2·46

Orientation of C–C bonds (°)

C(1,i)–C(1′,i) ∧ [100]	102·0 (1)	C(1,i)–C(1′,i) ∧ (100)	12·4 (1)
[010]	45·2 (1)	(010)	44·8 (1)
[001]	133·1 (1)	(001)	42·7 (1)
		(10$\bar{1}$)	13·7 (1)
C(1,i)–C(1′,i) ∧ C(1,vi)–C(1′,vi)	90·5		

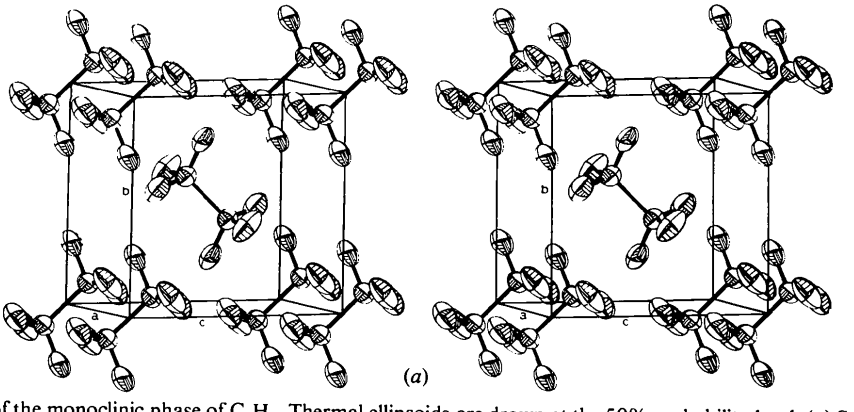

(*a*)

Fig. 5. Packing of the monoclinic phase of C_2H_6. Thermal ellipsoids are drawn at the 50% probability level. (*a*) Stereopicture.

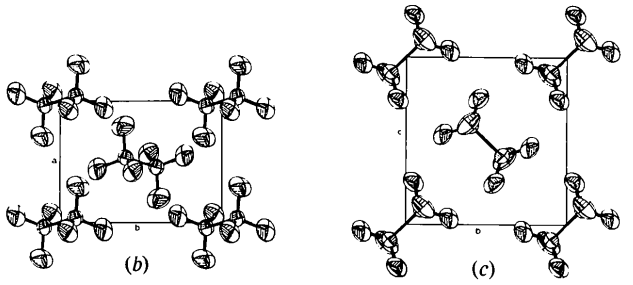

Fig. 5 (*cont.*). Projections of the structure (*b*) along [001] on (001), and (*c*) along [100] on (100).

(*c*) *Comparison with the Mark & Pohland* (1925) *structure*

Although some pseudo-hexagonal geometry can be distinguished in our monoclinic structure, Fig. 6 shows that our structure is strongly different from Mark & Pohland's (1925) hexagonal structure. In the monoclinic structure the centres of the molecules do not form a hexagonal arrangement and the C–C bonds of the two molecules in the cell are almost perpendicular and not parallel to each other. That the two structures are different is also clear from the fact that Mark & Pohland's (1925) powder diffraction data, especially the intensities of the reflexions, cannot be reconciled with our diffraction data. Attempts to achieve this by considering their sample as a mixture of monoclinic and cubic ethane also failed. The latter assumption was tested because the density of their sample, $D_m = 0{\cdot}694$ g cm^{-3}, lies between that of the cubic ($D_x = 0{\cdot}669$ g cm^{-3}) and the monoclinic ($D_x = 0{\cdot}719$ g cm^{-3}) modification. In view of Mark & Pohland's (1925) observation, it is not impossible that ethane has more than two solid modifications above 85 K.

PMR spectra of solid ethane have generally been interpreted on the basis of the Mark & Pohland (1925) structure (Givens & McCormick, 1977, and references therein). From the line-width variations as a function of temperature, the authors have deduced that the H atoms are rapidly reorienting about their C–C bonds and that the C–C bonds exhibit a strong libration (or even a reorientation) around axes perpendicular to the bond above 75 K. The thermal parameters found for our monoclinic structure only indicate (strong) libration around C–C. In view of the fact that Mark & Pohland's (1925) structure is very different from the present monoclinic structure, the interpretations of the PMR spectra are probably not completely correct.

6.2. *Twinning of the monoclinic crystals*

As shown in Fig. 5 and Table 4, the C–C bonds lie approximately in the *bc* plane. From the schematic drawing of Fig. 7, we see that the packing of the C–C bonds has pseudo orthorhombic symmetry (space group *Pmnn*) rather than only the monoclinic symmetry $P2_1/n$. This indicates that the individuals of the crystal twinned according to (001) (§ 3.3) may be related by an (approximate) glide plane *n* perpendicular to **c** (Fig. 8). This does not give rise to H···H distances shorter than the van der Waals distance at the twin boundary. Slight readjustment of ethane molecules at the boundary to avoid possible short intermolecular distances is not necessary.

Consideration of the structure in the *bc* plane (Fig. 7) shows that the C–C arrangement has even pseudo tetragonal symmetry (space group $P4_2/m\ 2_1/n\ 2/m$).

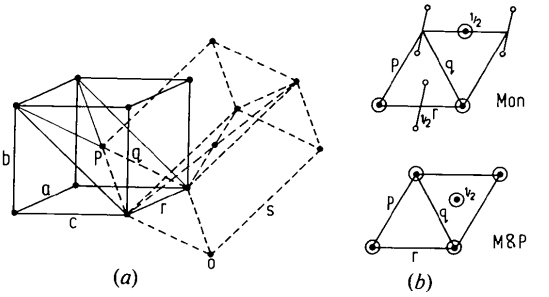

Fig. 6. Comparison between the monoclinic and Mark & Pohland's (1925) (M&P) structure. (*a*) Bold lines: monoclinic cell (p = 4·58, q = 4·56, r = 4·23, s = 8·11 Å); dashed lines: pseudo-hexagonal cell. Deviations in angles from 'hexagonal' values up to 5°; a(M&P) = 4·46, c(M&P) = 8·19 Å. (*b*) Schematic projection on the (pseudo) hexagonal base plane for the monoclinic structure (above) and the M&P structure (below). ⊙ = C–C ∥ **s** (hexagonal); heights of molecular centres along **s** are indicated.

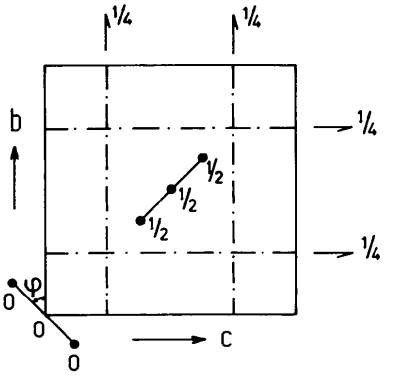

Fig. 7. Schematic drawing of the C–C bonds in the structure for $\beta = 90°$ and C–C parallel to (100) (symmetry *Pmnn*, No. 58, with $m \perp$ **a**). Further assumption of $b = c$ and $\varphi = 45°$ (see Fig. 5 and Table 4) gives symmetry $P4_2/m\ 2_1/n\ 2/m$ (No. 136 with 4_2 parallel to **a** and $m \perp$ **a**).

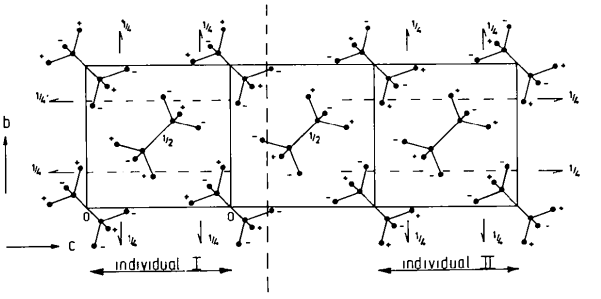

Fig. 8. Schematic view along **a** of twin boundary in the case when individuals (I) and (II) are related by glide plane *n* perpendicular to **c** for β (assumed) = 90°. + or − at H atoms indicates whether the C–H bonds of the molecule concerned are pointing up or down.

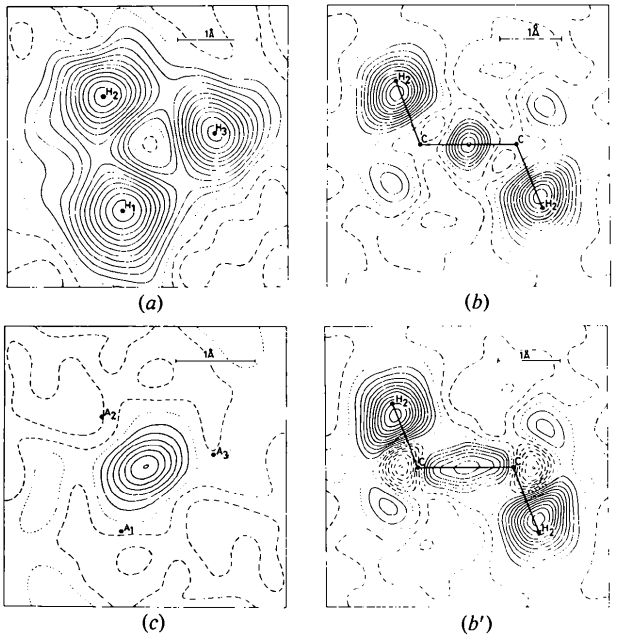

Fig. 9. Sections of difference density after refinement with C atoms only (see text). Sections (*a*), (*b*) and (*c*) calculated after refinement *A*2; (*b'*) after refinement *A*3. (*a*) Plane of H atoms perpendicular to C–C and at a distance of 1·167 Å from molecular centre (Fig. 4). (*b*), (*b'*) Plane H(2)–C–C–H(2). The H(2) positions marked in the figure are obtained from refinement *B*3. (*c*) Plane perpendicular to C–C through bond centre. Triangle A_1, A_2, A_3 is the projection of H(1), H(2), H(3) along C–C in the plane of (*c*). Contours are at intervals of 0·05 e Å^{-3}. Full lines are positive, dotted lines zero and dashed lines negative contours.

Therefore, quadruplet formation with individuals related by a pseudo 4_2 axis parallel to **a** is possible. It cannot be excluded that the existence of quadruplets is (partly) responsible for the additional peaks in our reflexion scans (§ 3.3), although this has not been evaluated further because of the very low intensities of these peaks.

6.3. *Discussion of electron density distributions for the monoclinic structure*

Sections of the $[F_o(H) - F_c(H,C)]$ map after ordinary unconstrained weighted refinement of the C atoms (model *A*2) are given in Fig. 9(*a*), (*b*) and (*c*). The section through the three H atoms clearly shows that these atoms have preferred positions around the C–C bonds. Around the centre of the C–C bond, the difference map shows a slightly elongated positive region with a maximum value of 0·35 (4) e Å^{-3}. This peak value may be compared with the values 0·32–0·37 e Å^{-3} observed for the 'bonding maxima' at the centres of the C–C single bonds in 2,5-dimethyl-3-hexyne-2,5-diol (Helmholdt & Vos, 1977*b*). Inclusion of H atoms in the refinement (model *B*2) does not have a marked influence around the C–C bond. To a good approximation, the section through the H atoms is flat in this case (highest absolute value 0·10 e Å^{-3}).

In contradistinction to the H(2)–C–C–H(2) section of Fig. 9(*b*) (C–C unconstrained) the H(2)–C–C–H(2) section of Fig. 9(*b'*) (C–C literature value) shows a slope at the position of the C atom. This slope is mainly due to the neglect of the librational character of the thermal motion in the *A*3 refinement.

Part of the research has been supported by the Dutch Organization for the Advancement of Pure Research (ZWO). The computations were carried out on the CYBER 74-16 computer of the University of Groningen.

References

BOLHUIS, F. VAN (1971). *J. Appl. Cryst.* **4**, 263–264.

CROMER, D. T. & MANN, J. B. (1968). *Acta Cryst.* A**24**, 321–324.

CRUICKSHANK, D. W. J. (1956). *Acta Cryst.* **9**, 754–756.

EGGERS, D. F. JR (1975). *J. Phys. Chem.* **79**, 2116–2118.

EGGERS, D. F. JR (1977). Private communication.

GIVENS, F. L. & MCCORMICK, W. D. (1977). *J. Chem. Phys.* **67**, 1150–1156.

HELMHOLDT, R. B. & VOS, A. (1977*a*). *Acta Cryst.* A**33**, 38–45.

HELMHOLDT, R. B. & VOS, A. (1977*b*). *Acta Cryst.* A**33**, 456–465.

HERZBERG, G. (1966). *Molecular Spectra and Molecular Structure*, Vol. II, p. 193. Princeton: Van Nostrand.

International Tables for X-ray Crystallography (1959). Vol. II, p. 324. Birmingham: Kynoch Press.

JOHNSON, C. K. (1969). *Acta Cryst.* A**25**, 187–194.

JOHNSON, C. K. (1970). *ORTEP*-II. Report ORNL-3794, second revision. Oak Ridge National Laboratory, Tennessee.

KUCHITSU, K. (1968). *J. Chem. Phys.* **49**, 4456–4462.

MARK, H. & POHLAND, E. (1925). *Z. Kristallogr.* **62**, 103–112.

NES, G. J. H. VAN & VAN BOLHUIS, F. (1978). *J. Appl. Cryst.* **11**, 206–207.

NES, G. J. H. VAN & VOS, A. (1977). *Acta Cryst.* B**33**, 1653–1654.

PAULING, L. (1960). *The Nature of the Chemical Bond*, 3rd ed., p. 260. Ithaca: Cornell Univ. Press.

PRESS, W. & ECKERT, J. (1976). *J. Chem. Phys.* **65**, 4362–4364.

SHMUELI, U. (1972). Chemistry Department, Univ. of Tel Aviv, Ramat-Aviv, Israel.

STEWART, R. F. (1976). *Acta Cryst.* A**32**, 565–574.

STEWART, R. F., DAVIDSON, E. R. & SIMPSON, W. T. (1965). *J. Chem. Phys.* **42**, 3175–3187.

STRATY, G. C. & TSUMURA, R. (1976). *J. Chem. Phys.* **64**, 859–861.

TEJADA, S. B. & EGGERS, D. F. JR (1976). *Spectrochim. Acta Part A*, **32**, 1557–1562.

WAHL, W. (1914). *Z. Phys. Chem.* **88**, 129–171.

WYCKOFF, R. W. G. (1966). *Crystal Structures*, Vol. 5, p. 225. New York: Interscience.

XRAY system (1975). Dutch version of the XRAY 72 system. Tech. Rep. TR-192, Computer Science Centre, Univ. of Maryland, College Park, Maryland.

ZACHARIASEN, W. H. (1967). *Acta Cryst.* **23**, 558–564.

ZACHARIASEN, W. H. (1968). *Acta Cryst.* A**24**, 212–216.